MEASUREMENT OF BEAM POLARISATION AND BEAM ENERGY IN ONE DEVICE*

N. Yu. Muchnoi†, Budker Institute of Nuclear Physics & Novosibirsk State University, Russia

Abstract

Electron beam interaction with the monochromatic laser radiation produces scattered photons and electrons due to the Compton effect. Both types of scattered particles carry the information about the polarisation (if any) and the energy of initial electrons in the beam. In this report we focus on the properties of the scattered electrons. After a bending magnet these electrons leave the beam and their X-Y space distribution is measured by the 2D pixel detector. We show that if the electron beam vertical emittance is sufficiently small, the shape of this distribution is an ellipse. Measurement of the length of the X-axis of this ellipse allow to calibrate accurately the bending field integral seen by the beam. The distribution of the electrons within the ellipse depends on the initial beam polarisation, allowing to measure the its degree and direction. So we propose a universal Compton polarimeter with a unique feature of precise calibration of the LEP-style beam energy spectrometer. The approach is thought to be useful for the future high-energy e+/e- colliders, while the feasibility tests may be performed on existing accelerators.

INTRODUCTION

An illustration for the process of Inverse Compton Scattering (ICS) is presented in Fig. 1:

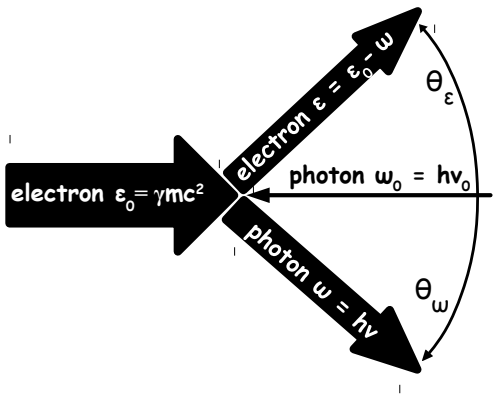

Figure 1: Inverse Compton scattering: the thickness of the arrows qualitatively represents the energies of the particles.

Considering the case when $\varepsilon_0, \varepsilon, \omega \gg \omega_0$ let's introduce the scattering parameter

$$u = \frac{\omega}{\varepsilon} = \frac{\theta_\varepsilon}{\theta_\omega} = \frac{\omega}{\varepsilon_0 - \omega} = \frac{\varepsilon_0 - \varepsilon}{\varepsilon}, \qquad (1)$$

where $u \in [0, \kappa]$ and $\kappa = 4\omega_0\varepsilon_0/mc^2$ is twice the ratio between the photon and electron energies in the electron rest frame. The photon and electron scattering angles are:

$$\eta_\omega \equiv \gamma\theta_\omega = \sqrt{\frac{\kappa}{u} - 1}; \quad \eta_\varepsilon \equiv \gamma\theta_\varepsilon = u\sqrt{\frac{\kappa}{u} - 1}. \qquad (2)$$

Further we consider an ICS of monochromatic laser radiation on the beam of ultra-relativistic electrons. ICS cross section is sensitive to the polarisation of initial electron and photon beams:

$$\frac{d\sigma}{du\, d\varphi} = \frac{r_e^2}{\kappa(1+u)^2}\times \qquad (3)$$

$$\times\left\{\left(2 + \frac{u^2}{1+u} + 4\frac{u}{\kappa}\left[\frac{u}{\kappa} - 1\right]\left[1 - \xi_\perp \cos(2(\varphi - \varphi_\perp))\right]\right) + \right.$$

$$\left. + \xi_\cup\left(\zeta_\parallel \frac{u(u+2)(\kappa - 2u)}{\kappa(1+u)} - \zeta_\perp \frac{2u^2\sqrt{\kappa/u - 1}}{\kappa(1+u)}\sin\varphi\right)\right\},$$

where

- φ is the azimuthal angle of scattered electron relative to horizon,
- $\xi_\perp$ and $\varphi_\perp$ are the degree and direction of laser beam linear polarisation,
- $\xi_\cup$ is the degree and sign of laser circular polarisation,
- $\zeta_\parallel$ and $\zeta_\perp$ are the signs and degrees of longitudinal and vertical transverse electron beam polarisations.

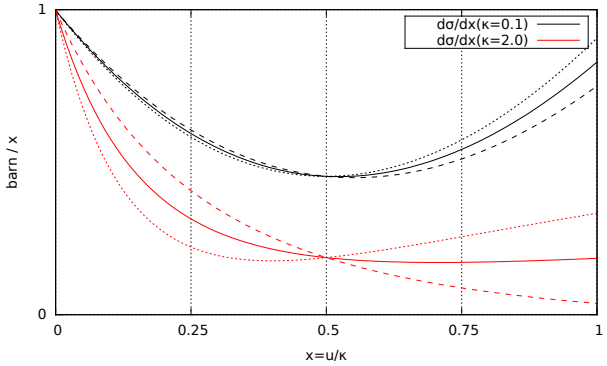

Figure 2: ICS cross section for small and large κ. The dashed lines illustrate the influence of $\xi_\cup\zeta_\parallel$.

Experiments with polarised $e^\pm$ beams were performed at many facilities (ACO, VEPP-2, SPEAR, DORIS, TRISTAN, VEPP-4, CESR, LEP, HERA...). Compton polarimeters usually dealt with scattered photons. General layout of ICS

* This work was supported by Russian Science Foundation (project N 14-50-00080)

† muchnoi@inp.nsk.su

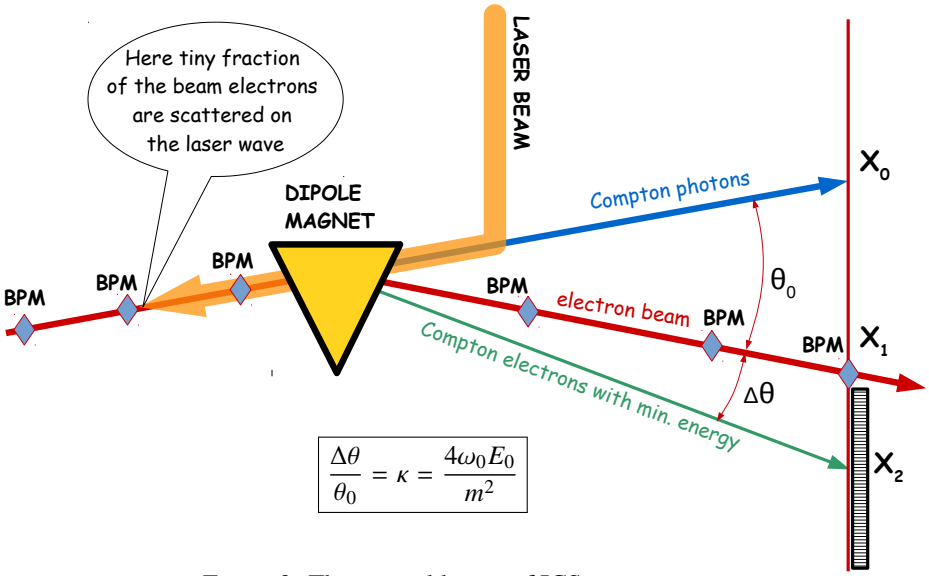

Figure 3: The general layout of ICS experiments.

experiments is shown in Fig. 3. At higher electron energies the divergence of γ-beam is small, high energy SR photons appear, etc. So it is reasonable (like ILC) to look at the scattered electrons. Maximum electron scattering angle: $\max(\theta_\varepsilon) = 2\omega_0/m$, see Eq. (2). It means that with ω_0 =2.33 eV one has $\max(\theta_\varepsilon) \simeq 10$ μrad. In order to distinguish kinematics of electrons at this angular range, the beam angular spread $\sigma'_y = \sqrt{\epsilon_y/\beta_y}$ should be much smaller than $\max(\theta_\varepsilon)$. For example, the parameters ϵ_y=100 pm and β_y=100 m gives $\sigma'_y = 1$ μrad. It's also important that the dimension of scattered electrons angular distribution does not depend on beam energy.

SCATTERED ELECTRONS AFTER A BENDING DIPOLE

An energy of a scattered electron depends on u as:

$$\varepsilon(u) = \varepsilon_0/(1+u). \tag{4}$$

This electron will be bent to the angle

$$\theta_s = \frac{c\int Bdl}{\varepsilon_0}(1+u), \tag{5}$$

where $\int Bdl$ is the field integral along the dipole (assuming it does not depend on electron energy). Let

$$\eta_s \equiv \gamma\theta_s = \eta_0 + u\eta_0, \tag{6}$$

where $\eta_0 = \int Bdl/B_c\lambda\!\!\!^{-}_c$ and $B_c\lambda\!\!\!^{-}_c$ is the product of Schwinger field and the Compton wavelength of an electron: $B_c\lambda\!\!\!^{-}_c = \dfrac{mc}{e} \simeq 1.7\times10^{-3}$ [T m]. With the scattered electron angles defined as

$$\begin{cases} \eta_x \equiv \eta_s - \eta_0 = u\eta_0 + & u\sqrt{\kappa/u-1}\cos\varphi \\ \eta_y = & u\sqrt{\kappa/u-1}\sin\varphi \end{cases} \tag{7}$$

one gets the equation:

$$(\eta_x - u\eta_0)^2 + \eta_y^2 = u(\kappa-u). \tag{8}$$

Equation 8 describes surface of determination for the ICS cross section, shown in Fig. 4 for $\kappa = 2$ and various η_0.

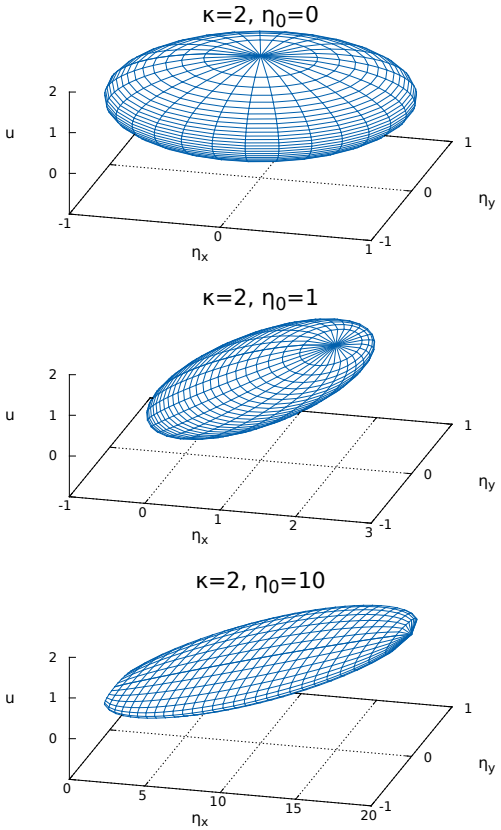

Figure 4: ICS surface in (u,η_x,η_y) space.

The scattered electrons distribution in the η_x, η_y plane can be obtained my Monte Carlo method, using Eq. (3) for game and Eq. (7) for tracking the scattered electrons through a dipole magnet. In Fig. 5 the results of such MC simulations are presented, and the shape of the ICS electrons in the η_x, η_y plane is an ellipse with certain dimensions. These dimensions, expressed in radians, are:

$$O_y = \frac{4\omega_0}{m}, \quad O_x = \frac{4\omega_0}{m}\sqrt{1+\eta_0^2} \tag{9}$$

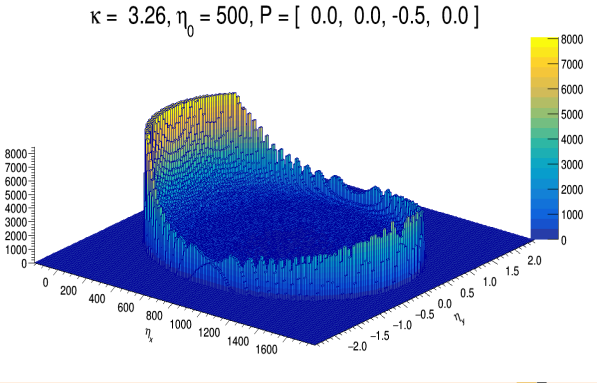

Figure 5: The scattered electrons distribution in η_x, η_y plane. $\kappa = 3.26$ when $\varepsilon_0 = 45.5$ GeV and $\omega_0 = 4.68$ eV. P is the polarisation vector and does not matter here. $\eta_0 = 500$ means that the electron beam was turned to an angle of $500 \cdot 1/\gamma$. Electron beam is located at $\eta_x = \eta_y = 0$.

In ref. [1] there is a study about application of silicon pixel detector to measure the distribution of scattered electrons, similar to one shown in Fig. 5, in order to determine the transverse polarisation of an electron beam in ILC. Based on this work is our assumption that there are existing apparatus allowing to measure such a distribution, and we're not going into details about it. In this report we want to show that the analysis of this distribution allows to measure whatever possible polarisation as well as to perform a precise calibration of magnetic spectrometer.

Our analysis is based on the procedure of fitting the 2D distribution of scattered electrons by the theory function. The cross section itself, according to Eq. (3), consists of tree parts. The new variables for the ICS cross section will be x and y, obtained by transformation of an ellipse, Eq. (9), to a circle where $x = y = 0$ is the centre of the circle. After some analytical calculations, Fig. 6 presents their results in graphical way. Three components of ICS cross section, according to Fig. 6 and its caption, are $\mathcal{U}$, $\mathcal{L}$ and $\mathcal{T}$. The distribution of scattered electrons in x, y coordinates is expressed by the convolution of

a) the cross section

$$f(x,y) = \mathcal{U} + \xi_{\cup}(\zeta_{\parallel}\mathcal{L} + \zeta_{\perp}\mathcal{T}) \tag{10}$$

b) transverse distributions (σ_x, σ_y) of beam electrons.

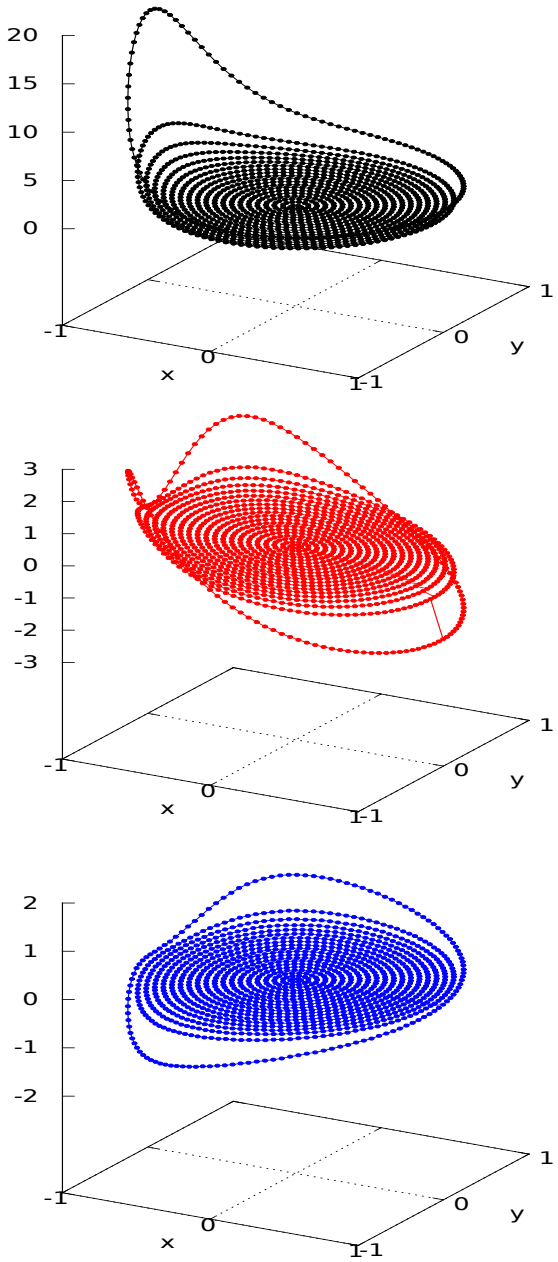

Figure 6: From top to bottom: three ICS cross section components: $\mathcal{U}$ - unpolarised (black), $\mathcal{L}$ - 100% longitudinal (red), $\mathcal{T}$ 100% transverse vertical (blue) e^-spin polarisation. Vertical scale (arbitrary units) is the same for all of the plots.

The horizontal (x) and vertical (y) dimensions of the components $\mathcal{U}$, $\mathcal{L}$ and $\mathcal{T}$ in Eq. (10) could be scaled to any real values of ω_0 and η_0 according to Eqs. (9). The only value, depending on the beam energy ε_0 is the value of the cross section at each point in Fig. 6. This dependence is relatively weak, see Fig. 2, so 10% accuracy in beam energy knowledge is more than enough for the fit success.

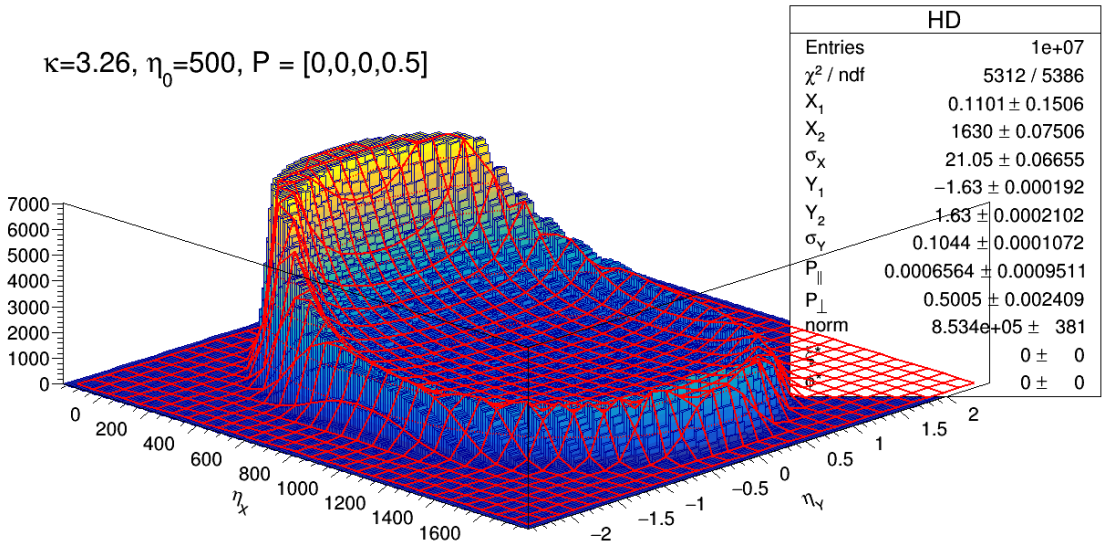

Figure 7: The MC distribution of scattered electrons with the fit function and fit results.

The example of fitted distribution is presented on Fig. 7. The initial conditions are:

- The horizontal size of an ellipse fixed by MC generator O_x equals $\kappa\eta_0 = 3.26 \cdot 500 = 1630$.
- $P = [0,0,0,0.5]$ is the polarisation vector meaning that $\xi_\perp = \varphi_\perp = \xi \cup \zeta_\parallel = 0$ and $\xi \cup \zeta_\perp = 0.5$.
- The histogram has 100 bins in η_x and 50 bins in η_y. In our consideration this is an equivalent of the number of detector pixels.
- The 10^7 scattered electrons were generated.
- Fit range in η_x is starting from $\eta_x = 200$, assuming that the smaller values of η_x are not available for measurement cause these electrons propagate too close to the beam. The electron beam itself is located at $\eta_x = \eta_y = 0$, see Fig. 3.
- the transverse horizontal an vertical sizes of the electron beam are described by Gaussian distributions with parameters $\sigma_x = 20$ and $\sigma_y = 0.1$ in the same units as η_0, η_x and η_y.

The fit results are shown in the parameters table in Fig. 7. The essential results are:

- $P_\parallel \equiv \xi \cup \zeta_\parallel = 0.0007 \pm 0.0009$.
- $P_\perp \equiv \xi \cup \zeta_\perp = 0.501 \pm 0.002$.
- $O_x \equiv X_2 - X_1 = (1630.02 \pm 0.08) - (0.110 \pm 0.151)$.

The polarisation parameter $P_\perp$ "was measured" with 0.4% accuracy. Note that X_1 is the beam position, which in principle can be also measured by beam position monitors, see Fig. 3. The relative error $\Delta X_2/(X_2 - X_1) \simeq 5 \cdot 10^{-5}$ in our example is twice better than the $\Delta X_1/(X_2 - X_1) \simeq 10^{-4}$. This is because the detector can not measure the part of the scattered electrons distribution close to the main beam, i. e., again, the fitting range in η_x is started at $\eta_x = 200$. We claim again that the O_x measurement is the measurement of the parameter $\eta_0 = \int Bdl/B_c\lambda_c$, i. e. the bending field integral. From the statistical point of view such measurement is evidently much more efficient to be compared to one-dimensional measurements of η_x only. The relative error in O_x measurement obviously depend on the number of detected particles (statistics) and the ratio between the overall size of the distribution and number of histogram bins (i. e. detector pixels). In this sense, the absolute value of $\kappa\eta_0 = 1630$ in our example, does not matter at all, the similar accuracy can be obtained for any other case.

The difference in trajectories of scattered and unscattered electrons

In all of the above considerations we have implicitly believed that the beam electrons and the scattered electrons are bent by the dipole in such a way, that all of these electrons experience the same bending force defined by the only one parameter $\eta_0 = \int Bdl/B_c\lambda_c$. However this is only an approximation, and electrons with different energies are propagating with individual trajectories. It is very important to understand the accuracy of this approximation. To do this, let us consider the possible difference of η_0 for the beam electrons with energy ε_0, and the scattered electrons with minimal energy $\varepsilon_{min} = \varepsilon_0/(1+\kappa)$. The bending radii of these electrons in the same bending field are related by:

$$R_{min} = R_0/(1+\kappa). \qquad (11)$$

In Fig. 8 the geometry of bending dipole is presented. By

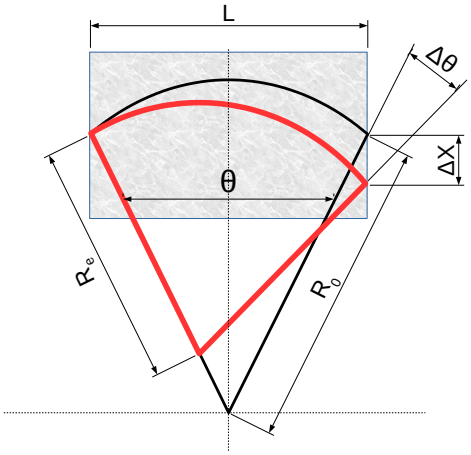

Figure 8: Bending of electrons with different energies. Black upper arc – the trajectory of en electron with ε_0 energy, red lower arc – the trajectory of en electron with ε_{min} energy.

simple trigonometry calculations one obtains:

$$S_0 = 2R_0 \arcsin\left[\frac{L}{2R_0}\right], \quad (12)$$

$$S = 2R_{min} \arcsin\left[\frac{\sqrt{L^2+\Delta X^2}}{2R_{min}}\right], \quad (13)$$

where

$$\Delta X = \sqrt{R_{min}^2 - \left[\frac{LR_{min}}{2R_0}\right]^2} - \sqrt{R_{min}^2 - \left[L - \frac{LR_{min}}{2R_0}\right]^2}.$$

We are going to compare the length of the trajectories $\Delta S = (S - S_0)/2S_0$ and the maximum transverse distance ΔX between trajectories in the spectrometer, illustrated by Fig. 9.

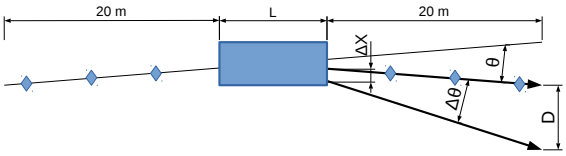

Figure 9: Sketch of spectrometer.

Table 1: Calculations by Eqs. (12, 13)

θ mrad	$\Delta\theta$ mrad	L m	ΔX mm	$\Delta S/S$	D mm
1	1.53	10	3.83	$2.59 \cdot 10^{-7}$	46
2	3.06	10	7.65	$1.04 \cdot 10^{-6}$	92
1	1.53	5	1.91	$2.59 \cdot 10^{-7}$	46
2	3.06	5	3.83	$1.04 \cdot 10^{-6}$	92

The results of calculations for various parameters are presented in Table 1, where D is the horizontal size of the distribution of scattered electrons at the detector. From Table 1 we see that our main approximation about the equality of η_0 for all electrons could be make rather strict by appropriate design of the spectrometer. It is also important to mention that

$$\Delta S/S \propto \kappa\theta, \quad \Delta X \propto \kappa\theta L, \quad D \propto \kappa\theta L_{arm}.$$

Since everything is proportional to $\kappa\theta$, our approximation is valid for any electron beam energy range. At high electron beam energies, implying circular machines, the value of θ is naturally small and the value of κ is naturally large. At low energies we can afford larger θ and will have smaller κ.

CONCLUSION

Inverse Compton scattering of laser radiation is a currently available reliable method for beam polarisation [2, 3] and energy [4–6] determination. The future high energy lepton colliders require polarised beams and polarimetry, inter alia for application of resonant depolarisation technique for precise beam energy calibration at circular machines. Analysis of 2D-distribution of ICS electrons allows to measure beam polarisation degree and direction as well as to provide a unique way for accurate calibration of the $\int Bdl$ exactly along a beam trajectory in a conventional magnetic spectrometer. Such a spectrometer was installed at LEP [7] and no doubt it should be implemented at future high-energy colliders, either linear or circular. The proposed approach has no limitations in beam energy, the only thing it requires is a small value of vertical emittance of the electron beam. Now it's a good time to start the proof-of-principle project at one of the existing low-emittance facilities. Another subject for further studies should be a possibility to measure the position of backscattered photons with high accuracy, see Fig. 3. This seems to be not an easy task, but it allows to build the completely independent beam energy measurement approach for arbitrary beam energies.

REFERENCES

[1] Itai Ben Mordechai and Gideon Alexander. ILC Note: LC-M-2012-001 (2012).

[2] M.Placidi, R.Rossmanith, Nucl. Instr. Meth. A274 (1989) 79-94.

[3] S.Boogert et al., JINST 4 P10015 (2009).

[4] V.E.Blinov et al., Nucl. Instr. Meth. A598 (2009) 23-30.

[5] E.V.Abakumova et al., Nucl. Instrum. Meth. A659 (2011) 21-29.

[6] E.V.Abakumova et al., Phys. Rev. Lett. 110 (2013) 140402.

[7] R.Assmann et al., Eur. Phys. J. C39 (2005) 253-292. SLD